First-Principles Photoemission Spectroscopy and Orbital Tomography in Molecules from Koopmans-Compliant Functionals

Ngoc Linh Nguyen,[1,*] Giovanni Borghi,[1] Andrea Ferretti,[2] Ismaila Dabo,[3] and Nicola Marzari[1]
[1]*Theory and Simulations of Materials (THEOS), and National Centre for Computational Design and Discovery of Novel Materials (MARVEL), École Polytechnique Fédérale de Lausanne, 1015 Lausanne, Switzerland*
[2]*Centro S3, CNR–Istituto Nanoscienze, 41125 Modena, Italy*
[3]*Department of Materials Science and Engineering, Materials Research Institute, and Penn State Institutes of Energy and the Environment, The Pennsylvania State University, University Park, Pennsylvania 16802, USA*
(Received 26 August 2014; published 24 April 2015)

The determination of spectral properties from first principles can provide powerful connections between microscopic theoretical predictions and experimental data, but requires complex electronic-structure formulations that fall outside the domain of applicability of common approaches, such as density-functional theory. We show here that Koopmans-compliant functionals, constructed to enforce piecewise linearity and the correct discontinuity derivative in energy functionals with respect to fractional occupation—i.e., with respect to charged excitations—provide molecular photoemission spectra and momentum maps of Dyson orbitals that are in excellent agreement with experimental ultraviolet photoemission spectroscopy and orbital tomography data. These results highlight the role of Koopmans-compliant functionals as accurate and inexpensive quasiparticle approximations to the spectral potential.

DOI: 10.1103/PhysRevLett.114.166405 PACS numbers: 71.15.Mb, 74.25.Jb, 79.60.-i

The interpretation of experimental spectra, such as those obtained with ultraviolet photoemission spectroscopy (UPS) or angular-resolved photoemission spectroscopy (ARPES), often requires theoretical support, due to the complexity of the data involved [1,2]. Theoretical predictions can help resolve spectral contributions coming from quasidegenerate excitations, allowing us to label each state with its native quantum numbers, or to find the correspondence between photoemission peaks and the probability density of the states from which electrons were emitted [3,4]. The power and accuracy of current experimental techniques, together with their microscopic resolution, strongly motivate the development of reliable first-principles methods able to reproduce accurately experimental spectra for different setups and photon energies, and to interpret them qualitatively and quantitatively. From a theoretical point of view, photoemission spectra have been studied with many-body perturbation theory [5,6], time-dependent extensions of density-functional theory (DFT) [7], density-matrix functional theory [8], or with the wave function methods of quantum chemistry [9,10]. However, due to the significant computational requirements of these approaches, and their own limits in terms of ultimate accuracy, applications are limited in system size and complexity. This is the reason why simpler methods such as Hartree-Fock or ground-state DFT are still frequently employed to interpret photoemission spectra [4,11].

Recently, Dabo and collaborators have introduced Koopmans-compliant (KC) functionals [12–16] to enforce a generalized criterion of piecewise linearity with respect to the fractional removal or addition of an electron from any orbital [and not only the highest occupation molecular orbital (HOMO)] in approximate DFT functionals, and to extend to the entire electronic manifold the self-interaction linearization imposed by DFT + Hubbard U [17,18]. The condition of Koopmans' compliance is naturally akin to that of enforcing a correct description of charged excitations, and thus can lead to orbital energies that are comparable to the quasiparticle excitations of photoemission experiments.

In this Letter, we illustrate the remarkable performance of the KC class of functionals in predicting ultraviolet photoemission spectra and orbital tomography momentum maps; such agreement with experiment is complemented by potential energy surfaces that preserve the quality of the base functionals [16], and by an accuracy for frontier orbital energies [ionization potentials (IPs) and electron affinities (EAs)] that is comparable and slightly superior to the state of the art in many-body perturbation theory, all at very moderate computational costs [16]. Crucially, these results support the view of Ref. [19] that KC functionals directly approximate the spectral potential, i.e., the local, frequency-dependent contraction of the electronic self-energy that is necessary and sufficient to describe the local spectral function [19,20] of a given system.

Photoemission spectra can be reproduced theoretically following the well-established three-step model, within the sudden approximation [2]. This approach treats the

photoexcitation as a transition from an electronic initial state $|\Phi_0^N\rangle$—which is the ground state with energy E_0^N—into an excited N-particle state $|\Phi_{i,\boldsymbol{k}}^N\rangle = |\Phi_i^{N-1}\rangle \otimes |\xi_{\boldsymbol{k}}\rangle$ of energy $E_{i,\boldsymbol{k}}^N$, composed of the ith excited state of the singly ionized system (with energy E_i^{N-1}) and the wave function $\xi_{\boldsymbol{k}}$ of the ejected electron, approximated by a plane wave of wave vector $\boldsymbol{k}$. The total photoemission intensity can be described, to first order in perturbation theory, through Fermi's golden rule [2] as

$$I^{(\nu)} \propto \sum_{i,\boldsymbol{k}} |\langle \Phi_0^N | \boldsymbol{A}\cdot\boldsymbol{p} | \Phi_{i,\boldsymbol{k}}^N\rangle|^2 \delta(h\nu + E_0^N - E_{i,\boldsymbol{k}}^N), \qquad (1)$$

which contains the squared modulus of the light-matter interaction operator in the dipole approximation—where $\boldsymbol{A}$ is the semiclassical electromagnetic field and $\boldsymbol{p}$ is the momentum operator of the electron. Equation (1) can be written in terms of single-particle Dyson orbitals $\phi_i^d(\boldsymbol{r}) = \langle \Phi_i^{N-1}|\hat{\Psi}(\boldsymbol{r})|\Phi_0^N\rangle$ and binding energies $E_i^b = E_i^{N-1} - E_0^N$, as [21]

$$I^{(\nu)} \propto \sum_{i,\boldsymbol{k}} |\langle \phi_i^d | \boldsymbol{A}\cdot\boldsymbol{p} | \xi_{\boldsymbol{k}}\rangle|^2 \delta\left(h\nu - E_i^b - \frac{\hbar^2\boldsymbol{k}^2}{2m}\right). \qquad (2)$$

More details on the calculation of $I^{(\nu)}$ can be found in the Supplemental Material [22]. The excitation energy is now expressed in terms of the kinetic energy $\hbar^2\boldsymbol{k}^2/2m$ of the ejected electron and its binding energy E_i^b defined as the negative of the Dyson orbital energy ε_i^d. The Dyson orbitals, whose energies are the poles of the one-body Green's function, fulfill the quasiparticle equation

$$[\hat{T} + \hat{\mathrm{v}} + \hat{\Sigma}(\varepsilon_i^d)]|\phi_i^d\rangle = \varepsilon_i^d |\phi_i^d\rangle, \qquad (3)$$

where $\hat{\mathrm{v}}$ is the sum of the external and Hartree potentials and $\hat{\Sigma}$ is the electron-electron self-energy, and can, in principle, be determined within the framework of many-body perturbation methods [5].

It has been argued [11,53] that exact KS eigenstates and eigenvalues can approximate Dyson orbitals and quasiparticle excitations, particularly when close to the HOMO. Nevertheless, approximate rather than exact density functionals display electronic eigenvalues that are only in poor correspondence with particle-removal energies; even the HOMO, that would be correctly reproduced by exact DFT, is typically underestimated due to self-interaction errors [15,54,55]. Self-interaction is also responsible for the spatial over-delocalization of charge density and wave functions [18,55], and a number of methods have been proposed to counteract it; these include the Perdew-Zunger correction (PZ) [54], DFT + Hubbard U [17,18], and range-separated hybrids [56,57]. Last, it is important to note that a local static potential does not provide the correct framework to define Dyson orbitals [5], which are solutions of the quasiparticle equation [Eq. (3)] in the presence of a nonlocal and frequency-dependent self-energy.

KC functionals, on the other hand, provide a formalism to approximate directly the spectral potential [19] and the quasiparticle excitations. These functionals are obtained by removing, orbital-by-orbital, the nonlinear (Slater) contribution to the energy as a function of fractional occupation and replacing in its lieu a linear (Koopmans) term, providing in a functional form some of the concepts present in Slater's ΔSCF approach. The linear term can be chosen either following Slater's suggestion [58], proportional to the orbital energy at half occupation (in which case the KC functional is labeled simply as K [13]), or as the difference between the energies of the two adjacent electronic configurations with integer occupation; this latter is labeled KI ("I" standing for "integral"). The numerical differences between these two functionals are negligible, and so we focus here on KI, that is more straightforward to implement, and on its combination with the Perdew-Zunger correction, that we label KIPZ. All these functionals, described in detail in Refs. [13,16,59], are obtained from an approximate functional E^{app} as $E^{\mathrm{app}} + \alpha\sum_i \Pi_i$, where for KI

$$\Pi^{\mathrm{KI}}(\rho_i) = -\int_0^{f_i} \langle\varphi_i|H^{\mathrm{app}}(s)|\varphi_i\rangle ds + f_i\int_0^1 \langle\varphi_i|H^{\mathrm{app}}(s)|\varphi_i\rangle ds, \qquad (4)$$

and for KIPZ

$$\Pi^{\mathrm{KIPZ}}(\rho_i) = \Pi^{\mathrm{KI}}(\rho_i) - f_i E_{\mathrm{Hxc}}[|\varphi_i|^2], \qquad (5)$$

respectively. In the above equations, $\rho_i = f_i|\varphi_i|^2$, and $H^{\mathrm{app}}(s)$ is the approximate KS Hamiltonian calculated with orbital φ_i occupied by a fractional amount s. The multiplicative factor $\alpha \in [0,1]$ in the definition of E^{KC} acts as a simplified electronic screening, and it is chosen so that the IP of a neutral molecule is equal to EA of the molecular cation (i.e., enforcing Koopmans' condition, see Refs. [13,56]). As shown by Dabo *et al.* [13,14] and Borghi *et al.* [16], this constant screening is sufficient to accurately predict IP and EA energies from the eigenvalue spectrum of a variety of molecular systems, although a more sophisticated orbital-dependent choice might be convenient in the case of more complex or extended systems (given that the electron affinities are a most challenging case, we will discuss here the effects of calculating the screening not only on neutral molecules, but also on the molecular anions, labeling these results as EA*).

The Koopmans orbital-by-orbital linearity condition imposed through Eqs. (4) or (5) leads to an orbital-density-dependent (ODD) formulation in which the energy functional depends on the density of the individual orbitals. As such, it is not invariant under unitary rotations [19,59–61] and the *variational orbitals* $|\varphi_i\rangle$ that minimize

the ODD functional are different from the eigenstates or *canonical orbitals* $|\phi_m\rangle$ that diagonalize it, as discussed, e.g., in Refs. [59–61]. The generalized eigenvalue equation is

$$\hat{H}^{\mathrm{app}}|\phi_m\rangle + \tilde{\Sigma}_m|\phi_m\rangle = \varepsilon_m|\phi_m\rangle, \tag{6}$$

with

$$\tilde{\Sigma}_m(\boldsymbol{r})\phi_m(\boldsymbol{r}) = \sum_i \hat{\mathrm{v}}_i(\boldsymbol{r})\varphi_i(\boldsymbol{r})U^{\dagger}_{im}, \tag{7}$$

where the unitary matrix U transforms the variational orbitals $|\varphi_i\rangle$ into the canonical ones $|\phi_m\rangle = \sum_i |\varphi_i\rangle U^{\dagger}_{im}$ and where $\hat{\mathrm{v}}_i(\boldsymbol{r}) = [\delta\Pi^{\mathrm{KC}}(\rho_i)/\delta\rho_i(\boldsymbol{r})]$. The similarity of Eq. (6) with the quasiparticle Eq. (3) is evident; we also note that the operator $\hat{\mathrm{v}}_i$ acts on the variational state $|\varphi_i\rangle$ as a simplified self-energy that is local or even constant in space (this is the case for the KIPZ and KI functionals, respectively). As discussed in Ref. [19], ODD canonical orbitals have a natural interpretation as Dyson orbitals, and their energies as particles' removal energies; this interpretation will be clearly supported by the results of the present work. In the limit of a crystalline system, the canonical orbitals satisfy Bloch's theorem, whereas the variational orbitals remain localized (and are actually very similar to maximally localized Wannier functions [62]), so that $\hat{\mathrm{v}}_i$ depends only on local properties, even in periodic crystals, and converges rapidly to its nontrivial thermodynamical limit—allowing seamless application to atoms, molecules, and solids [currently, the only requirement for Eq. (6) to be well defined is that the system under consideration has a finite gap, which ensures that the filling of variational orbitals is either zero or one, and the definition of orbital densities ρ_i unambiguous]. We also note in passing that, using this terminology, the ensemble-DFT correction of Ref. [63] is equivalent to the KI functional, but applied to the canonical orbitals rather than the variational ones.

First, we highlight in Fig. 1 and Table I the accuracy of the KC functionals in predicting the energy of frontier orbitals, by comparing IPs and EAs for a set of 23 photovoltaic molecules; KI and KIPZ show a performance which is comparable to the state of the art of many-body perturbation methods. For reference, we also provide Slater ΔSCF results, that are known to be good estimates for the frontier energies of molecular systems; we also note that ΔSCF corrections will go to zero in extended systems [64], while KI and KIPZ rapidly converge to their thermodynamic limit. We next show in Fig. 2 a comparison of the photoemission spectra for three gas-phase molecules (pentacene, porphine and fullerene C_{60}), confirming how these KC functionals can successfully predict the binding energies of deeper states and the correct photoemission amplitudes. Indeed, the three panels of Fig. 2 display a remarkable agreement between the predicted KI and KIPZ spectra and the experimental data (extensive results for all 23 molecules of Fig. 1 and at different photon energies are shown in the Supplemental Material [22]). The improvement is evident not only in the peak positions, but also in the shapes and intensities.

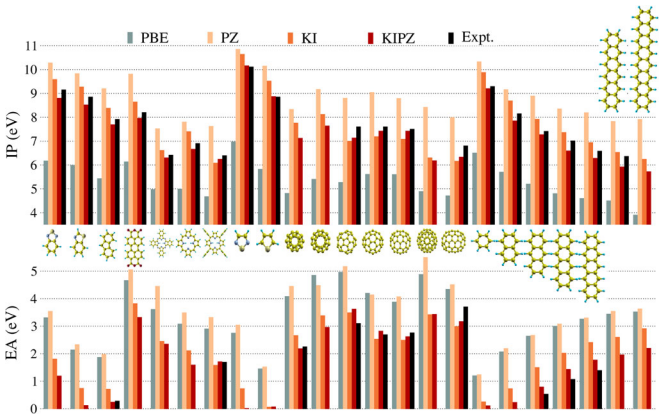

FIG. 1 (color online). IPs and EAs for 23 organic photovoltaic molecules, obtained from the energies of the frontier orbitals and calculated using either PBE or the self-interaction corrected functionals PZ, KI, and KIPZ (all using PBE as base), and compared with available experimental data.

We believe there are two main explanations for the accuracy of these functionals: (i) KI corrects the KS eigenvalues of approximate DFT by aligning them to particle removal energies through Koopmans' condition, while (ii) KIPZ adds to this feature the exactness in the one-electron limit, in which it recovers the Rydberg series of the hydrogen atom. This latter property (i.e., recovering the $1/r$ behavior of the exact KS potential) is essential in the development of novel functionals and plays an important role in the prediction of fundamental gaps and excitation energies [57]. At variance with the KI functional, the KIPZ functional is able to modify not only the electronic excitation energies of approximate DFT, but also the manifold of electronic orbitals (i.e., the single-particle density-matrix) [16]. A change in the density matrix has repercussions on the values of both the photoemission peak intensity and the position of every electronic excitation, which allows the KIPZ functional to yield a more accurate description of experimental data. Notably, KC functionals

TABLE I. Mean absolute errors with respect to experiments for the IPs (16 molecules, in eV) and EAs (10 molecules, in eV) for the molecules of Fig. 1, for which experimental and self-consistent *GW* data are available (see Table I and II of the Supplemental Material [22], and Refs. [23,24]). We also show results obtained with a screening factor appropriate to the molecular anion, rather than the neutral molecule (these are labeled EA*).

	PBE	PZ	KI	KIPZ	ΔSCF	scf-*GW*
IP	2.26	1.27	0.45	0.25	0.35	0.31
EA	1.62	1.82	0.50	0.22	0.22	0.29
EA*			0.22	0.17		

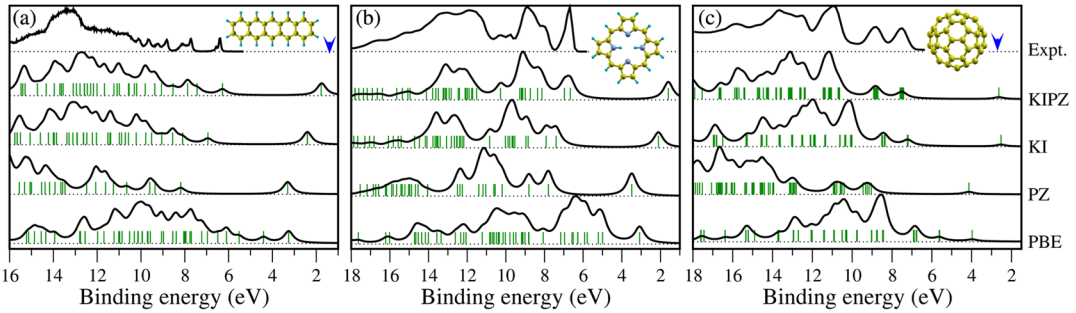

FIG. 2 (color online). UPS spectra for (a) pentacene, (b) porphine, and (c) fullerene C_{60} calculated using the PBE, PZ, KI, and KIPZ functionals, and plotted as a function of electron binding energy $h\nu - \hbar^2k^2/(2m)$. For pentacene and porphine the calculations are done for an incoming photon energy of 21.22 eV (corresponding to the experimental HeI radiation), and are compared with experimental gas-phase UPS measurements using HeI (Ref. [25] and Ref. [26]), while for fullerene C_{60} calculations and experimental data (Ref. [27]) are for a 50 eV photon energy. The blue arrows mark the experimental electron affinities (corresponding to the binding energy of the lowest unoccupied molecular orbital) of pentacene and C_{60}, taken from Refs. [28] and [29].

are successful also in capturing the change in photoemission peak positions and intensities when changing the energy of the incoming photon. Figure 3 displays, for instance, the results for fullerene C_{70}, compared with experiments, for incident photon energies of 21.22 (Ref. [27]) and 50 eV (Ref. [30]), showing again a very good agreement between theoretical and experimental spectra for peak positions and relative intensities. Also, it is known that the first three peaks of the spectrum of C_{70} are subject to pronounced variations as a function of the energy of the incident photon $h\nu$, with the relative intensities of the first two peaks showing characteristic oscillations (see Ref. [30] and references therein) that are described very accurately by our formulation in the entire 0–200 eV range (see inset of Fig. 3).

In the last part of this Letter, we discuss the ability of KC functionals to predict data obtained from orbital tomography [65]. This technique consists in exploiting angle-resolved photoemission spectroscopy to extract momentum maps of molecular orbitals [4,66]. Because of the complexity of spectroscopic data, the deconvolution of orbital maps from photoemission results requires the support of theoretical UPS simulations [4]. Unfortunately, the accuracy of approximate DFT is particularly compromised in systems whose ground-state wave function is composed of KS eigenstates with very different spatial character, e.g., localized versus delocalized. This difference in localization is such that different eigenstates carry unequal self-interaction biases, so that even the orbital ordering disagrees with experiments. An example of this can be found in NTCDA (1,4,5,8-naphthalene-tetracarboxylic dianhydride) in which localized orbitals on the anhydride side groups and delocalized ones on the naphthalene core coexist at close orbital energies [67]. In NTCDA,

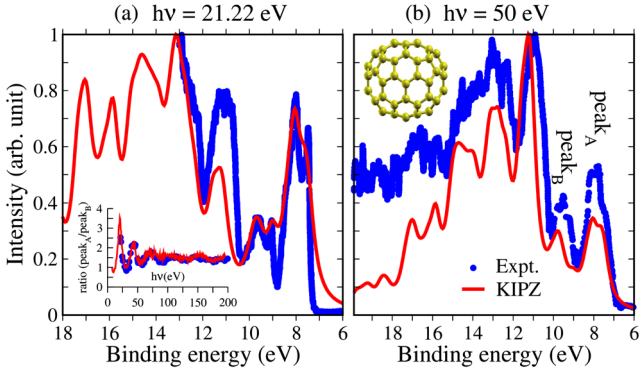

FIG. 3 (color online). Theoretical predictions for the photoemission spectrum of fullerene C_{70}, performed at incoming photon energies of (a) 21.22 and (b) 50 eV. These are compared with experimental gas-phase photoemission data at the same photon energies, taken from Refs. [27] and [30], respectively. The inset in (a) shows the photoemission intensity ratio of the A and B peaks computed at different photon energies, using the KIPZ functional (red line); the experimental data (blue dots) are taken from Ref. [30].

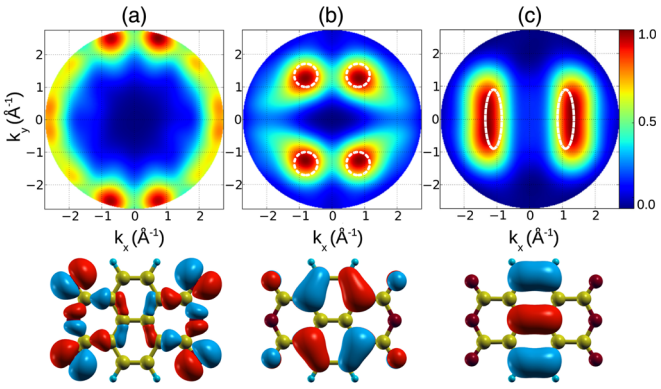

FIG. 4 (color online). Square of the Fourier transforms of different molecular orbitals in NTCDA, as computed with different methods: (a, top) HOMO, PBE, (b, top) HOMO, KIPZ, and (c, top) HOMO-1, KIPZ. White dashed circles in the (k_x, k_y)-momentum maps represent experimental intensity isolines taken from Ref. [66]. The bottom of each panel shows the charge density isosurfaces corresponding to their respective orbitals, color coded according to the sign of the wavefunctions.

energy differences are smaller than the self-interaction errors on two of the lowest-lying localized orbitals, so that in PBE these are pushed higher in energy—up to the HOMO and the HOMO-1. These assignments contradict experimental results [see Fig. 4(a)] and accurate studies combining ARPES data and a generalized optimized effective potential approach, with which Dauth *et al.* [66] demonstrate that HOMO and HOMO-1 should correspond to two delocalized orbitals with an energy difference of about $\Delta E = 0.44$ eV (measured from the experimental kinetic energy difference of photoelectrons ejected from either state). We find that the KIPZ functional not only predicts the correct ordering and maps of the orbitals [see Figs. 4(b) and 4(c)], but also a correct energy difference of $\Delta E = 0.41$ eV.

In conclusion, we have shown in this Letter the accuracy of Koopmans-compliant functionals [12–16] in describing spectral properties from first principles; these properties include ionization potentials, electron affinities, ultraviolet photoemission spectra, and orbital tomography momentum maps, all in close agreement with experimental measurements. While the results presented here have focused on molecules, the rapid convergence of the localized variational orbitals to their bulk thermodynamic limit allows a direct extension of these concepts to the case of extended systems. As argued in Ref. [19], these functionals introduce a beyond-DFT approach where the spectral potential, rather than the exchange-correlation one, is directly approximated, and provide both a conceptual and a practical framework to predict spectral properties from functional theories, rather than perturbative approaches.

*linh.nguyen@epfl.ch

[1] S. Hüfner, *Photoelectron Spectroscopy: Principles and Applications* (Springer, Berlin, Heidelberg, 1996).

[2] A. Damascelli, Z. Hussain, and Z.-X. Shen, Rev. Mod. Phys. **75**, 473 (2003).

[3] N. Stojić, A. Dal Corso, B. Zhou, and S. Baroni, Phys. Rev. B **77**, 195116 (2008).

[4] P. Puschnig, S. Berkebile, A. J. Fleming, G. Koller, K. Emtsev, T. Seyller, J. D. Riley, C. Ambrosch-Draxl, F. P. Netzer, and M. G. Ramsey, Science **326**, 702 (2009).

[5] G. Onida, L. Reining, and A. Rubio, Rev. Mod. Phys. **74**, 601 (2002).

[6] M. Guzzo, G. Lani, F. Sottile, P. Romaniello, M. Gatti, J. J. Kas, J. J. Rehr, M. G. Silly, F. Sirotti, and L. Reining, Phys. Rev. Lett. **107**, 166401 (2011).

[7] U. De Giovannini, D. Varsano, M. A. L. Marques, H. Appel, E. K. U. Gross, and A. Rubio, Phys. Rev. A **85**, 062515 (2012).

[8] S. Sharma, J. K. Dewhurst, S. Shallcross, and E. K. U. Gross, Phys. Rev. Lett. **110**, 116403 (2013).

[9] Y. R. Huang, C. G. Ning, J. K. Deng, and M. S. Deleuze, Phys. Chem. Chem. Phys. **10**, 2374 (2008).

[10] O. Dolgounitcheva, V. G. Zakrzewski, and J. V. Ortiz, J. Chem. Phys. **134**, 074305 (2011).

[11] D. P. Chong, O. V. Gritsenko, and E. J. Baerends, J. Chem. Phys. **116**, 1760 (2002).

[12] I. Dabo, PhD thesis, MIT, Cambridge MA, 2008, http://dspace.mit.edu/handle/1721.1/44320; I. Dabo, M. Cococcioni, and N. Marzari, arXiv:0901.2637v1.

[13] I. Dabo, A. Ferretti, N. Poilvert, Y. Li, N. Marzari, and M. Cococcioni, Phys. Rev. B **82**, 115121 (2010).

[14] I. Dabo, A. Ferretti, C.-H. Park, N. Poilvert, Y. Li, M. Cococcioni, and N. Marzari, Phys. Chem. Chem. Phys. 2013) 685 ,**15**).

[15] I. Dabo, A. Ferretti, G. Borghi, N. L. Nguyen, N. Poilvert, C. H. Park, M. Cococcioni, and N. Marzari, Psi-K Newsletter **119**, 1 (2013); I. Dabo, A. Ferretti, and N. Marzari, Topics Current Chem. **347**, 193 (2014).

[16] G. Borghi, A. Ferretti, N. L. Nguyen, I. Dabo, and N. Marzari, Phys. Rev. B **90**, 075135 (2014).

[17] M. Cococcioni and S. de Gironcoli, Phys. Rev. B **71**, 035105 (2005).

[18] H. J. Kulik, M. Cococcioni, D. A. Scherlis, and N. Marzari, Phys. Rev. Lett. **97**, 103001 (2006).

[19] A. Ferretti, I. Dabo, M. Cococcioni, and N. Marzari, Phys. Rev. B **89**, 195134 (2014).

[20] M. Gatti, V. Olevano, L. Reining, and I. V. Tokatly, Phys. Rev. Lett. **99**, 057401 (2007).

[21] M. Walter and H. Häkkinen, New J. Phys. **10**, 043018 (2008).

[22] See Supplemental Material at http://link.aps.org/supplemental/10.1103/PhysRevLett.114.166405 for the data shown in Fig. 1 and Table I, details on the calculation of UPS spectra, and its performance for 23 molecules relevant for photovoltaic applications, which includes Refs. [4,19,23,24,25–29,30,31–52].

[23] X. Blase, C. Attaccalite, and V. Olevano, Phys. Rev. B **83**, 115103 (2011).

[24] M. L. Tiago, P. R. C. Kent, R. Q. Hood, and F. A. Reboredo, J. Chem. Phys. **129**, 084311 (2008).

[25] V. Coropceanu, M. Malagoli, D. A. da Silva Filho, N. E. Gruhn, T. G. Bill, and J. L. Brédas, Phys. Rev. Lett. **89**, 275503 (2002).

[26] P. Dupuis, R. Roberge, and C. Sandorfy, Chem. Phys. Lett. **75**, 434 (1980).

[27] D. L. Lichtenberger, M. E. Rempe, and S. B. Gogosha, Chem. Phys. Lett. **198**, 454 (1992).

[28] L. Crocker, T. Wang, and P. Kebarle, J. Am. Chem. Soc. **115**, 7818 (1993).

[29] X.-B. Wang, C.-F. Ding, and L.-S. Wang, J. Chem. Phys. **110**, 8217 (1999).

[30] S. Korica, A. Reinkäster, M. Braune, J. Viefhaus, D. Rolles, B. Langer, G. Fronzoni, D. Toffoli, M. Stener, P. Decleva, O. Al-Dossary, and U. Becker, Surf. Sci. **604**, 1940 (2010).

[31] Y. Li and I. Dabo, Phys. Rev. B **84**, 155127 (2011).

[32] J. P. Perdew, K. Burke, and M. Ernzerhof, Phys. Rev. Lett. **77**, 3865 (1996).

[33] The norm-conserving pseudopotentials for C, O, S, N, and H were taken from the Quantum ESPRESSO pseudopotential download page: http://www.quantum-espresso.org/pseudo.php.

[34] S. Klüpfel, P. Klüpfel, and H. Jónsson, Phys. Rev. A **84**, 050501 (2011).

[35] *NIST Chemistry WebBook, NIST Standard Reference Database Number 69*, edited by P. J. Linstrom and

W. G. Mallard (National Institute of Standards and Technology, Gaithersburg MD, 2015), http://webbook.nist.gov.
[36] N. Dori, M. Menon, L. Kilian, M. Sokolowski, L. Kronik, and E. Umbach, Phys. Rev. B **73**, 195208 (2006).
[37] J. Berkowitz, J. Chem. Phys. **70**, 2819 (1979).
[38] T. Pasinszki, M. Krebsz, and G. Vass, J. Mol. Struct. **966**, 85 (2010).
[39] J. A. Zimmerman, J. R. Eyler, S. B. H. Bach, and S. W. McElvany, J. Chem. Phys. **94**, 3556 (1991).
[40] M. N. Piancastelli, M. K. Kelly, Y. Chang, J. T. McKinley, and G. Margaritondo, Phys. Rev. B **35**, 9218 (1987).
[41] D. Biermann and W. Schmidt, J. Am. Chem. Soc. **102**, 3163 (1980).
[42] H. Prinzbach, F. Wahl, A. Weiler, P. Landenberger, J. Wrth, L. T. Scott, M. Gelmont, D. Olevano, F. Sommer, and B. von Issendorff, Chem. A Eur. J. **12**, 6268 (2006).
[43] S. Yang, C. Pettiette, J. Conceicao, O. Cheshnovsky, and R. Smalley, Chem. Phys. Lett. **139**, 233 (1987).
[44] X.-B. Wang, H.-K. Woo, X. Huang, M. M. Kappes, and L.-S. Wang, Phys. Rev. Lett. **96**, 143002 (2006).
[45] J. Schiedt and R. Weinkauf, Chem. Phys. Lett. **266**, 201 (1997).
[46] P. Giannozzi *et al.*, J. Phys. Condens. Matter **21**, 395502 (2009).
[47] G. M. Seabra, I. G. Kaplan, V. G. Zakrzewski, and J. V. Ortiz, J. Chem. Phys. **121**, 4143 (2004).
[48] S.-Y. Liu, K. Alnama, J. Matsumoto, K. Nishizawa, H. Kohguchi, Y.-P. Lee, and T. Suzuki, J. Phys. Chem. A **115**, 2953 (2011).
[49] N. O. Lipari and C. B. Duke, J. Chem. Phys. **63**, 1768 (1975).
[50] E. Clar, J. M. Robertson, R. Schloegl, and W. Schmidt, J. Am. Chem. Soc. **103**, 1320 (1981).
[51] D. Löffler, S. S. Jester, P. Weis, A. Böttcher, and M. M. Kappes, J. Chem. Phys. **124**, 054705 (2006).
[52] T. Cummins, M. Bürk, M. Schmidt, J. Armbruster, D. Fuchs, P. Adelmann, S. Schuppler, R. Michel, and M. Kappes, Chem. Phys. Lett. **261**, 228 (1996).
[53] M. E. Casida, Phys. Rev. A **51**, 2005 (1995).
[54] J. P. Perdew and A. Zunger, Phys. Rev. B **23**, 5048 (1981).
[55] A. Cohen, P. Mori-Sanchez, and W. Yang, Science **321**, 792 (2008).
[56] T. Stein, H. Eisenberg, L. Kronik, and R. Baer, Phys. Rev. Lett. **105**, 266802 (2010).
[57] S. Refaely-Abramson, S. Sharifzadeh, N. Govind, J. Autschbach, J. B. Neaton, R. Baer, and L. Kronik, Phys. Rev. Lett. **109**, 226405 (2012).
[58] J. C. Slater, *Quantum Theory of Molecules and Solids: The Self-Consistent Field for Molecules and Solids* (McGraw-Hill, New York, 1963).
[59] G. Borghi, C.-H. Park, A. Ferretti, N. L. Nguyen, and N. Marzari, Phys. Rev. B **91**, 155112 (2015).
[60] D. Hofmann, S. Klüpfel, P. Klüpfel, and S. Kümmel, Phys. Rev. A **85**, 062514 (2012).
[61] S. Lehtola and H. Jónsson, J. Chem. Theory Comput. **10**, 5324 (2014).
[62] N. Marzari, A. A. Mostofi, J. R. Yates, I. Souza, and D. Vanderbilt, Rev. Mod. Phys. **84**, 1419 (2012).
[63] E. Kraisler and L. Kronik, Phys. Rev. Lett. **110**, 126403 (2013).
[64] R. W. Godby and I. D. White, Phys. Rev. Lett. **80**, 3161 (1998).
[65] We use the terminology orbital tomography to conform to the current literature; we stress that it is the square of the Fourier transform of the Dyson orbitals that is measured.
[66] M. Dauth, T. Körzdörfer, S. Kümmel, J. Ziroff, M. Wiessner, A. Schöll, F. Reinert, M. Arita, and K. Shimada, Phys. Rev. Lett. **107**, 193002 (2011).
[67] T. Körzdörfer, S. Kümmel, N. Marom, and L. Kronik, Phys. Rev. B **79**, 201205 (2009).